Measurement of Rapid Release Kinetics for Drug Delivery

Uwe Pliquett,[1] Mark R. Prausnitz,[2] Yuri A. Chizmadzhev,[3] and James C. Weaver[1,4]

Received June 27, 1994; accepted November 11, 1994

A fluorescence measurement system and methods of data analysis were developed to measure rapid kinetics of transdermal transport in vitro. Three variations on the technique were demonstrated, where the receptor compartment concentration was determined by: 1) fluorescence measurements of aliquots removed at discrete time points, 2) continuous fluorescence measurements made directly in the receptor compartment using a custom-made fluorimeter cuvette as a permeation chamber, and 3) continuous fluorescence measurements made in a flow-through cuvette containing receptor solution continuously pumped from a flow-through permeation chamber. In each case, the measured signal was a convolution of the time-dependent molecular flux (the desired information) and the characteristic response of the measurement system. Algorithms for deconvolution of the signal were derived theoretically. For the most complicated case, (3), the experimental confirmation is shown here, proving a time resolution on the order of half a minute.

KEY WORDS: transdermal drug delivery; fluorescence measurements; deconvolution; flow-through system; electroporation; percutaneous transport.

INTRODUCTION

Experimental determination of molecular fluxes across physical and biological barriers is critical to the development of new drug delivery techniques, including transdermal drug delivery (1,2). As a result, measurement of transport kinetics using flow-through, or continuous sampling methods has been introduced for characterizing release profiles for pharmaceutical tests (3,4). Moreover, flow-through systems have been characterized (5–8) and mathematical analysis has been performed for transdermal drug delivery systems where the contents of the receptor compartment are flowed continuously to an automated fraction collector (6–8). Mathematical analysis has also been performed for collection methods involving removal of aliquots from the receptor compartment (9).

These approaches, which involve the collection of samples at discrete time points, are limited in time resolution, as they become cumbersome for large numbers of sample times. In this study, we describe methods, with accompanying mathematical analysis, for measuring transdermal flux with time resolution on the order of a half minute. This work was motivated largely by the need to more accurately measure the rapid kinetics of transdermal transport by electroporation (10,11). However, the approach can be applied to many other situations where rapid release kinetics need to be assessed.

This study has investigated transdermal flux enhancement using "high voltage" pulses, which may create transient aqueous pathways within stratum corneum lipids by a mechanism involving electroporation (10–13). To partially characterize these pathways, we chose to study transport of calcein, a moderately sized (623 g/mol), hydrophilic, charged ($z = 4$), fluorescent molecule (14). We have used fluorescent molecules, because they offer: (a) high sensitivity of fluorescence measurements, (b) low toxicity, (c) broad choice of water/lipid solubility, and (d) selection of parameters such as size, charge, and fluorescent properties.

To determine molecular flux across skin, the concentration in the receptor compartment of a permeation chamber was measured as a function of time. The flux was then calculated using algorithms presented here. Although the measurement methods and algorithms are general, their specific application to measurement of rapid transdermal transport due to electroporation is demonstrated. This approach yielded average fluxes computed with a time resolution on the order of a half minute, which is adequate for many transdermal drug delivery studies.

MATERIALS AND METHODS

In this study, three different permeation systems were used: 1) a side-by-side permeation chamber (Fig. 1; Crown Glass, Somerville, NJ), from which aliquots were removed at discrete time points, 2) a custom-made fluorimeter cuvette, or micro-chamber (Fig. 2), containing skin as well as flow-through donor and receptor solutions, and 3) a side-by-side flow-through permeation chamber from which receptor solution was continuously pumped through a fluorimeter cuvette. Heat-stripped human epidermis (1,2) was placed in a permeation chamber, where the donor compartment faced the stratum corneum and the receptor compartment faced the viable epidermis. The exposed area of skin was 0.7 cm^2 (side-by-side permeation chamber) or 0.4 cm^2 (micro-chamber). Both donor and receptor compartments contained well-stirred phosphate-buffered saline (PBS, pH 7.4; Sigma, St. Louis, MO). The donor compartment also contained 1 mM calcein (Sigma).

For studies where time resolution was less important, removal of aliquots from the receptor compartment (volume = 3.5 ml) of a side-by-side chamber was performed. Fluorescence of aliquots was measured in a spectrofluorimeter (Fluorolog-2, model F112AI, SPEX Industries, Metuchen, NJ).

The fastest time resolution was achieved with a micro-chamber, in which both pulsing and measuring took place within the fluorimeter (Fig. 2). Both sides of the chamber were flow-through compartments, where the flow inlet was located at the bottom of the chamber and the outlet was located at the top. The receptor compartment was illuminated by an excitation beam (488 nm), while fluorescent emission (515 nm) was measured by a photomultiplier tube.

[1] Harvard-MIT Division of Health Sciences and Technology, Massachusetts Institute of Technology, Cambridge, Massachusetts 02139.
[2] Department of Chemical Engineering, Massachusetts Institute of Technology, Cambridge, Massachusetts 02139.
[3] Russian Academy of Science—Frumkin Institute of Electrochemistry, Leninsky Prospect, 31 Moscow, V-71 Russia.
[4] To whom correspondence should be addressed.

0724-8741/95/0400-0549$07.50/0

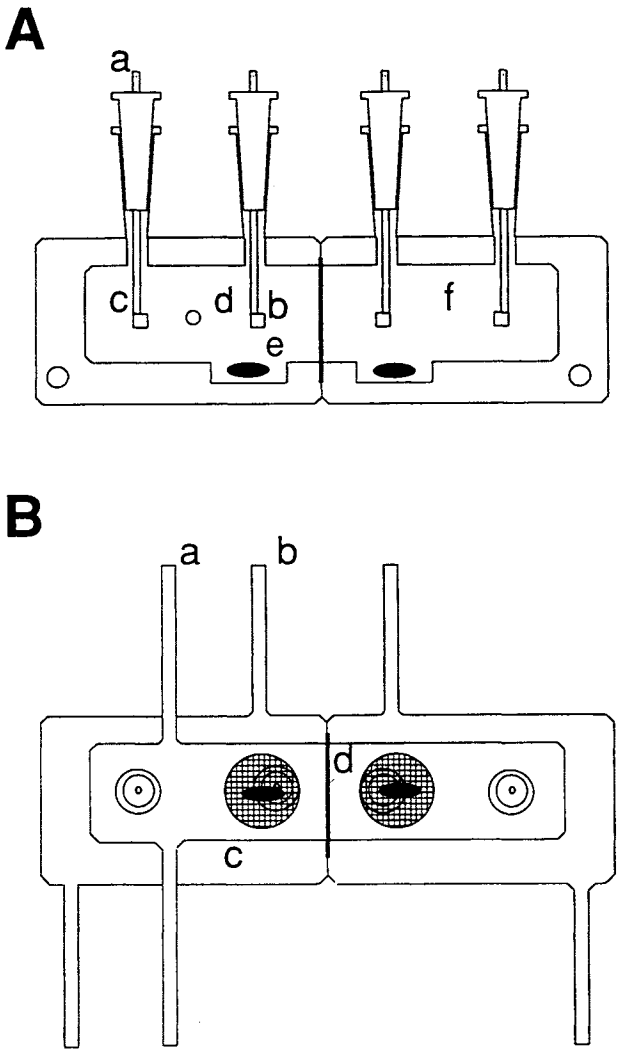

Fig. 1. Side-by-side permeation chamber. This chamber is designed to hold four electrodes, two of which apply the electrical protocols and two of which measure skin electrical properties. The receptor compartment is well mixed and contains an inlet and outlet allowing flow-through capabilities for continuous measurement of receptor compartment fluorescence. A) Side view: contacts for electrodes (a), inner electrodes for measurement of skin electrical properties (b), outer electrodes for application of electrical protocols (c), flow-through receptor compartment (d), magnetic stir bar (e), and donor compartment (f). B) Top view: inlet and outlet for flow-through (a), ports for water jacket (b), water jacket (c), and skin (d).

To prevent loss of fluorescence intensity in the small donor compartment (22 μl), fresh donor solution was continuously provided (~10 μl/s).

A third permeation system was used to simplify the protocol, while still allowing good time resolution. A side-by-side flow-through permeation chamber, containing an inlet and outlet at the receptor chamber (volume = 3.5 ml), permitted continuous sampling (Fig. 3). In this case, the fluorimeter was placed downstream from the chamber to continuously measure receptor solution fluorescence. A sample stream flow rate of 50–100 ml/h provided good time resolution while maintaining a high signal-to-noise ratio. To minimize mixing in the tubing before fluorescence was measured, tubing between the permeation chamber and fluorimeter was short (26 cm), thin (0.6 mm inner diameter), and made of Teflon, selected because of its low friction and chemical inertness. The flow-through cuvette inside the fluorimeter was designed with a small volume (200 μl) to reduce error associated with subsequent deconvolution.

Tests of the system, involving fast injections, were performed using only the receptor compartment (a piece of latex was placed between the donor and receptor compartments, instead of skin). 100 μl of 1 mM calcein was quickly (<1 s) injected into the receptor compartment and fluorescence was then measured in the fluorimeter over time.

When pulsing protocols were used, electric field pulses (exponential-decay time constant, τ_{pulse} = 1.1 ms; GenePulser, BioRad, Richmond, CA) were applied with Ag/AgCl electrodes (In Vivo Metrics, Healdsburg, CA), each located 3 cm from the skin, as described previously (10). Reported voltages are transdermal values.

THEORETICAL MODELING AND SIGNAL DECONVOLUTION

The measured fluorescence signal obtained from the

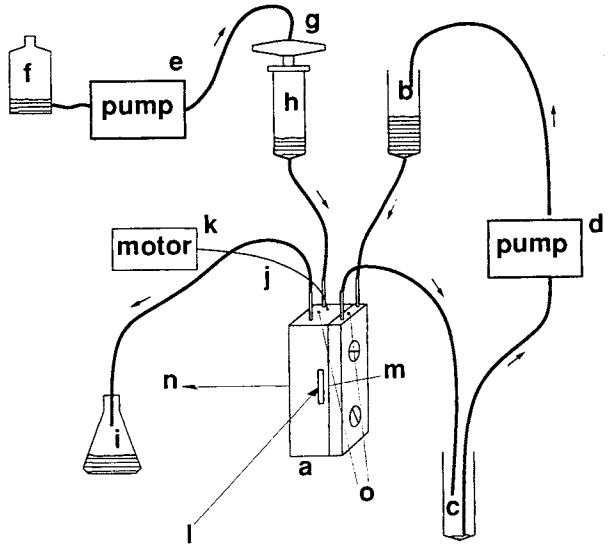

Fig. 2. Schematic of a flow-through system using a micro-chamber (a), with which fluorescence was measured and pulses were applied directly inside the fluorimeter. Both sides of the chamber were flow-through compartments, to provide fresh solutions continuously. The donor stream contained 1 mM calcein fed by gravity from a supply dish (b), to the donor compartment. Donor solution then emptied into a holding dish (c) and was recycled to the supply dish with a peristaltic pump (d). The receptor stream (containing PBS) was driven by a peristaltic pump (e) from a supply dish (f) through a filter (0.2 μm) (g) and an air-buffered dish (h) to the micro-chamber. Pressure differences across the skin were eliminated by adjusting the height of the air-buffered dish. Receptor solution leaving the micro-chamber was emptied into a waste dish (i). The receptor compartment contained a stirrer (j) powered externally by a motor (k). A polarized excitation beam (l) entered the receptor compartment parallel to the skin (m), while fluorescent emission (n) was collected at 90°. The micro-cuvette contained two silver pulsing electrodes with external contacts (o) and was painted black to reduce noise from stray light, except for two windows left clear for excitation and emission beams.

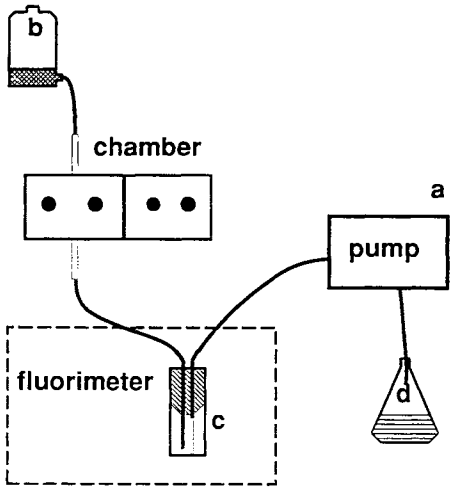

Fig. 3. Schematic of a flow-through system using a side-by-side chamber. Receptor solution (containing PBS), driven by a peristaltic pump (a), was fed from a supply dish (b), into the receptor compartment of the chamber (see Fig. 1), through a flow-through cuvette (c) in the fluorimeter, and emptied into a waste dish (d). PBS feeding the receptor compartment was degassed to reduce both formation of air bubbles and fluorescence bleaching due to oxygen radicals. Because changes in the level of PBS in the supply dish influenced the receptor stream flow rate, the PBS level was maintained constant by periodically adding PBS using a small water pump.

fluorimeter is a convolution of (a) the characteristic function of the system and (b) the transdermal flux. In other words, the measured fluorescence is a function not only of the rate of transdermal transport, but also of the mixing and pumping times of the measurement system. In order to deconvolute this signal, we needed to know the characteristic function of the system (i.e., the effects of mixing and pumping). First, a mass balance was performed on the receptor compartment and known parameters were independently measured (e.g., receptor compartment volume, skin surface area). This yielded an expression which could be used to deconvolute the signal to calculate the average transdermal flux. Then, the validity of this expression was verified by convoluting the calculated characteristic function of the system and a known input (e.g., an almost instantaneous injection of a known amount of fluorescent compound into the receptor compartment). The predicted and experimental signal versus time profiles were then compared to establish whether the system had been correctly characterized.

Fluorescence Measurements of Aliquots Made at Discrete Time Points

Only one method for taking aliquots was performed in our experiments and considered here. The entire receptor compartment solution was removed for analysis and replaced with fresh buffer. The fluorescence of each aliquot represents the amount of fluorescent molecule transported across the skin between t_{n-1} (time of previous aliquot) and t_n (time of current aliquot, Table I provides symbol definitions):

$$c = \frac{A}{V}\int_{t_{n-1}}^{t_n} J(t)dt \tag{1}$$

To correlate the fluorescence signal obtained from the fluorimeter with absolute molecule concentration, a calibration curve must be generated over the linear range of the fluorimeter, resulting in a proportionality factor, $k_f = c/F$, where concentration can be expressed on a molar, molecular, or mass basis.

The average flux between t_{n-1} and t_n is

$$\bar{J} = \frac{cV}{A \cdot (t_n - t_{n-1})} = \frac{k_F FV}{A\,\Delta t} \tag{2}$$

Data for this kind of measurement are shown in Ref. 10.

Continuous Fluorescence Measurements Made Directly in the Receptor Compartment

Using the microchamber (Fig. 2), fluorescence measurements were made directly in the receptor compartment. Unlike the case of removing aliquots at discrete time points, the microchamber receptor solution was continuously removed and replaced with fresh buffer. Thus, the mass balance on the receptor compartment is

$$V\frac{dc(t)}{dt} = A \cdot J(t) - \omega \cdot c(t) \tag{3}$$

In this equation, V represents a perfectly mixed receptor compartment volume, ω is the volumetric rate of plug flow (no mixing) in the tubing, and $J(t)$ is the molecular flux into the receptor compartment, which, in the specific case of transdermal delivery, represents efflux from the epidermis. Under these assumptions, the flux, $J(t)$, can be calculated from measured values of $c(t)$. With this in mind, it is convenient to rewrite Eq. 3 for fluorescence measurements made at discrete times,

$$\overline{J_n} = \frac{1}{A}\left(\frac{V\,\Delta c_n}{\Delta t} + \omega\,\overline{c_n}\right) \tag{4}$$

where $\Delta c_n = c_n - c_{n-1}$, $\overline{c_n} = (c_{n-1} + c_n)/2$ and $\overline{J_n}$ is the average flux between t_{n-1} and t_n. From Eq. 4 it is possible to

Table I. Definition of Symbols

c	average concentration of molecules
k_F	proportionality factor between fluorescence signal and concentration
m	injection number
n	aliquot or measurement number
t	time
Δt	time between measurements
A	area for transport (skin)
F	fluorescence emission intensity
J	molecular flux
N	number of molecules
T	time between injections
V	volume
τ	residence time (V/ω)
τ_{pulse}	time constant of the applied electrical pulse
τ_{pump}	time for transport between receptor and fluorimetercuvette
ω	volumetric flow rate within tubing

calculate the molecular flux ($\overline{J_n}$) for the microchamber as a function of the concentration in the receptor compartment.

Continuous Fluorescence Measurements Made in a Cuvette Containing Solution Pumped from the Receptor Compartment

From hydrodynamic point of view the system, containing a side-by-side permeation chamber and a flow through cuvette is an extension of the microchamber system (Fig. 3). The mass balance on the flow-through fluorimeter cuvette is

$$\frac{dc_2(t)}{dt} = \frac{\omega}{V_2} \cdot c_1(t) - \frac{\omega}{V_2} \cdot c_2(t) \tag{5}$$

where the subscript 1 is used for the receptor compartment and 2 for the fluorimeter cuvette. Using Eq. 5 to express $c_1(t)$ as a function of $c_2(t)$ and known constants and substituting the resulting expression for $c(t)$ in Eq. 7, the mass balance for receptor compartment, yields

$$J(t) = \frac{1}{A}\left(\frac{V_1V_2}{\omega}\frac{d^2c_2(t)}{dt^2} + (V_1 + V_2)\frac{dc_2(t)}{dt} + \omega c_2(t)\right) \tag{6}$$

By measuring $c_2(t)$ in the fluorimeter, Eq. 6 can be used to find $J(t)$. For measurements made at discrete times, separated by a constant interval, Δt, the flux is

$$\overline{J_n} = \frac{1}{A}\left(\frac{V_1\Delta c_{1_n}}{\Delta t} + \frac{\omega(c_{1_n} + c_{1_{n+1}})}{2}\right) \tag{7}$$

Here, $\Delta c_{1_n} = c_{1_n} - c_{1_{n-1}}$, where

$$c_{1_n} = \frac{V_2(c_{2_n} - c_{2_{n-1}})}{\Delta t\omega} + \frac{c_{2_{n-1}} + c_{2_n}}{2} \tag{8}$$

and

$$c_{1_{n-1}} = \frac{V_2(c_{2_{n-1}} - c_{2_{n-2}})}{\Delta t\omega} + \frac{c_{2_{n-2}} - c_{2_{n-1}}}{2} \tag{9}$$

This analysis assumes that the transit time from the receptor compartment to the cuvette (τ_{pump}) is much smaller than the time between measurements (Δt). If this is not the case, the time-axis should be shifted by τ_{pump}, which equals the tubing volume divided by the volumetric flow rate.

Response of the System to a Known Input. We verified the model by predicting the system response to a known input, a δ-function. That is, we measured the fluorescence injection of a known amount of fluorescent molecule (calcein) into the receptor compartment. This response was then compared to the prediction made, based on the equations derived below. Because the system containing the side by side permeation chamber and the fluorimeter cuvette is an extension of the microchamber system, and is more complicated, we focus by verifying our data on this system. After an instantaneous δ-function input, the system within the receptor compartment is described by

$$\frac{dc_1}{dt} + \frac{\omega}{V_1}c_1 = 0 \tag{10}$$

with $c_{1,0} = N/V_1$ as the initial condition immediately after injection. The solution yields

$$c_1(t) = c_{1,0} \cdot e^{-\frac{t}{\tau_1}} = \frac{N}{V_1} \cdot e^{-\frac{t}{\tau_1}} \tag{11}$$

where $\tau_1 = V_1/\omega$, representing the residence time of the receptor compartment.

Considering multiple injections, numbered from 1 to m and regularly spaced by an interval, T, the concentration between injections is

$$c_1(mT^+ + t) = \frac{1}{V_1}\sum_{i=1}^{m} N_i \cdot e^{-\frac{(m-i)T+t}{\tau_1}} \tag{12}$$

where t is the time since the previous injection (at mT) and N_i is the number of molecules introduced during the ith injection. To distinguish between conditions immediately before and after an injection, the respective notations mT^- and mT^+ are used.

We now consider the case where each injection introduces the same amount of fluorescent molecule. Solution of Eq. 10 with the boundary condition, $c_1(mT^+) = N/V_1 + c_1(mT^-)$, yields an expression for the concentration between the injections m and $m + 1$

$$c_1(mT^+ + t) = \left(\frac{N}{V_1} + c_1(mT^-)\right)e^{-\frac{t}{\tau_1}} \tag{13}$$

A quasi-steady state occurs when the number of molecules which leave the chamber between two injections equals the number of molecules introduced by each injection. In this case, $c_1(mT^-) = c_1((m + 1)T^-)$ and

$$\omega\int_0^T c_1(t)dt = N \tag{14}$$

From Eqs. 13 and 14, we obtain

$$c_1(mT^-) = \frac{N}{V_1}\frac{e^{-T/\tau_1}}{(1 - e^{T/\tau_1}} \tag{15}$$

Solving Eq. 5, using $c(t)$ in Eq. 11 for the concentration in the receptor compartment, $c_1(t)$, yields

$$c_2(t) = \frac{N}{V_1 - V_2}\left(e^{-\frac{t}{\tau_1}} - e^{-\frac{t}{\tau_2}}\right) \tag{16}$$

where $\tau_1 = V_1/\omega$, $\tau_2 = V_2/\omega$, and $N = C_{1,0}V_1$.

Considering multiple injections, numbered from 1 to m and spaced by a constant interval, T, the concentration between injections is

$$c_2(mT^+ + t) = \frac{1}{V_1 - V_2}\sum_{i=1}^{m} N_i\left(e^{-\frac{(m-i)T+t}{\tau_1}} - e^{-\frac{(m-i)T+t}{\tau_2}}\right) \tag{17}$$

To solve for the quasi-steady state concentration, Eq. 13 is substituted into Eq. 5, yielding

$$\frac{dc_2(t)}{dt} = \frac{1}{\tau_2}\left(\frac{N}{V_1} + c_1(mT^-)\right)e^{-t/\tau_1} - \frac{1}{\tau_2}c_2(t) \tag{18}$$

which can be rewritten, using Eq. 15, as

$$\frac{dc_2(t)}{dt} + \frac{1}{\tau_2} c_2(t) = \frac{N}{\tau_2 V_1} \frac{e^{-t/\tau_1}}{1 - e^{-T/\tau_1}} \tag{19}$$

The solution for this differential equation is

$$c_2(MT^+ + t) = e^{-t/\tau_2} \left[\frac{N\tau_1}{V_1(\tau_1 - \tau_2)(1 - e^{-T/\tau_1})} \cdot e^{\frac{(\tau_1 - \tau_2)t}{\tau_1\tau_2}} + C \right] \tag{20}$$

where C is the constant of integration. Substituting Eq. 20 into Eq. 14 gives

$$C = \frac{-N}{(V_1 - V_2)(1 - e^{-T/\tau_2})} \tag{21}$$

Finally, substituting C into Eq. 20 gives

$$c_2(mT^+ + t) = \frac{N}{V_1 - V_2} \left(\frac{e^{-t/\tau_1}}{1 - e^{-T/\tau_1}} - \frac{e^{-t/\tau_2}}{1 - e^{-T/\tau_2}} \right) \tag{22}$$

which represents the concentration inside the fluorimeter cuvette between two injections during the quasi steady state.

RESULTS AND DISCUSSION

Although all three types of fluorescence measurement were performed, here the side-by-side permeation chamber was emphasized for the purpose of confirming theoretical assumptions and evaluating the data. Data for the aliquot experiments are shown in Ref. 10. The fluorescence vs. time profiles obtained from the fluorimeter were convolutions of the transdermal flux and the characteristic response function of the measurement system (i.e., the effects of mixing and pumping). Using the equations developed in the previous section, the fluorescence signal can be deconvoluted to obtain the average transdermal flux.

Figure 4 shows both the fluorescence signal (Fig. 4A) and the fluorescence signal which has been deconvoluted to yield the transdermal flux obtained (Fig. 4B). The differences between the curves indicate the importance of deconvolution for the correct determination of transdermal flux. In Figure 4A, the convoluted signal contains information about transdermal flux as well as other kinds of transport inherent to the measurement system. In Figure 4B, the data has been deconvoluted to remove many of the effects of transport processes inherent to the measurement apparatus (i.e., mixing and pumping times) and averaged over 10 s to reduce noise. The visible oscillation in the Figure 4B are due to the pulsing protocol (1 ppm).

To assess the accuracy of the model used for deconvolution, the characteristic function of the system was used to predict fluorimeter cuvette concentration vs. time profiles, which were then compared to experimental results. The response to a δ-function input was modeled and measured experimentally by rapidly injecting a known amount of calcein into the receptor compartment (Fig. 5). The side-by-side, flow-through chamber was used, since its analysis is the most complex and therefore the most rigorous test.

There is approximate agreement between the predicted

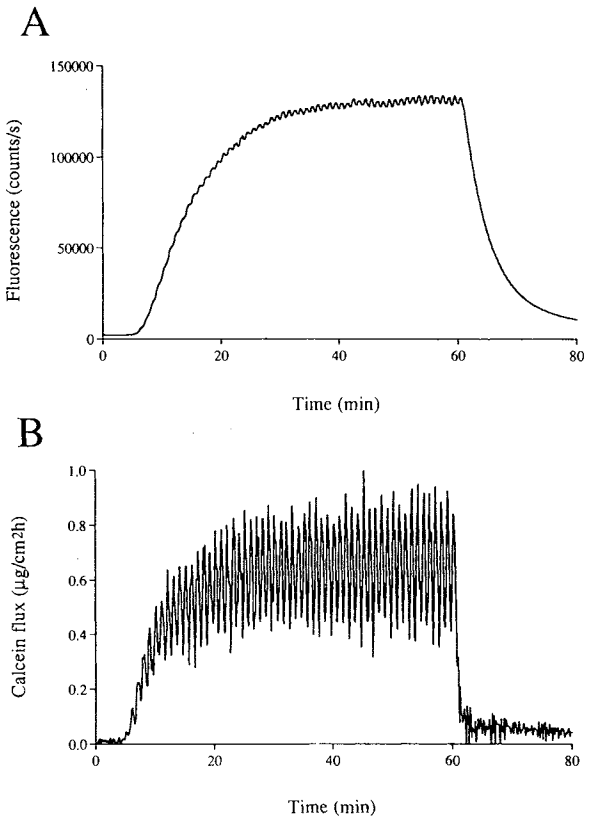

Fig. 4. (A) Measured fluorescence and (B) deconvoluted transdermal flux. Exponential-decay pulses (320 V, τ_{pulse} = 1.1 ms) were applied at a rate of 1 pulse per minute, using a side-by-side flow-through permeation chamber.

concentration and that measured experimentally, indicating that the general characteristics of the experimental system were correctly modeled. However, there are discrepancies between the curves, suggesting that some of the more subtle characteristics of the system were not adequately represented. This probably includes imperfect fluorimeter cuvette mixing, as well as imperfect receptor chamber mixing, small time variations of tube flow rates, and deviations from plug flow in the tubing. The error associated with these effects

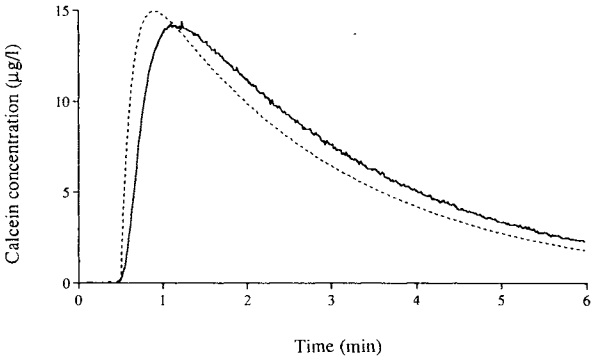

Fig. 5. Verification of system charcterization in the side-by-side flow-through chamber. Measured (solid line) and predicted (dashed line) concentrations inside the fluorimeter cuvette are shown after instantaneous injection of 100 μl of 1 μM calcein into the receptor compartment.

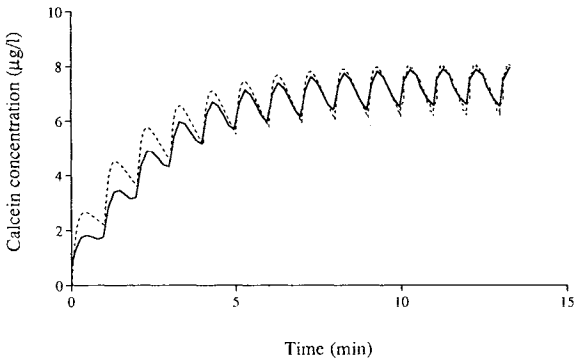

Fig. 6. The two plots compare a completely mathematical result to an experimental measurement. The dotted line is the purely theoretical behavior (theoretical prediction) for a series of evenly spaced δ-function inputs using Eq. 17 and $N_i = 1.07 \times 10^{12}$ (11.03 ng). This is a good approximation for the periodic transport of calcein across the skin, because the pulse duration (τ_{pulse}) is 1 ms, which is much slower than the about one-half minute time resolution of the system, and also slower than the interval between pulses (1 min). This allows a direct comparison with the measurements (solid line) for a multiple pulse protocol using 1 ms pulses spaced at intervals of one minute.

appears to result in a systematic shift in the time axis on the order of 10 s.

Given this uncertainty, the deconvolution can only quantitatively correct for charcteristic times greater than about one half minute. For example, the steady state lag time determined from the convoluted data (Fig. 4A) of 13 min was corrected by deconvolution (Fig. 4B) to 8 min. Moreover, the occurrence of time-periodic variations in flux at a rate of 1 per minute is also quantitatively correct. However, the exact time scale of the transient behavior during each oscillation, having characteristic times on the order of 10 s, is not correctly measured, because of the uncertainty of the time resolution of the system.

This approach may assist studies of transdermal transport by electroporation. Electroporation-mediated transport across cell membranes and other lipid bilayers is believed to occur predominantly by electrically-driven transport (i.e., electrophoresis and/or electroosmosis) during pulses (11,12). If this is also the case in skin, then for millisecond pulses and fluorescence measurements made every second, transport by electroporation could be modeled as a δ-function input occurring at the time of each pulse. Using the model developed for a series of δ-function inputs, Figure 6 shows the predicted and measured time profiles for electroporation pulses applied to skin once per minute. The approximate agreement between the two curves suggests that a δ-function can be used to model transdermal transport by electroporation. However, there is significant overprediction of the amount of calcein transported by each pulse during the first pulses. Thus, transport by electroporation may occur in skin mainly by electrically-driven transport during pulses, where the amount transported by each pulse is a function of time.

The above comparison between measured data and δ-function inputs indicates that transport due to each pulse occurred over a time scale of seconds or less. In contrast, the deconvoluted data in Figure 4B suggests that each pulse caused transport over a characteristic time on the order of 10 s. However, given the 10 s uncertainty associated with the system characterization, we are unable to distinguish between a δ-function input and a 10 s input. Thus, Figures 4B and 6, along with an understanding of electroporation in other systems, suggest that transport due to each pulse occurred over a time scale on the order of 10 s or less.

Here, theoretical models have been developed for three versions of our measurement system. If time resolution of hours or longer is needed, removal of aliquots may be the simplest approach (analysis governed by Eq. 2). However, if better time resolution is needed, the aliquot method becomes cumbersome. Flow-through apparati are useful for faster measurement, where the microchamber should give better resolution than the side-by-side, flow-through chamber (respective analyses governed by Eqs. 4 and 7.) However, the microchamber requires special construction and care during operation.

A good combination of rapid time resolution and ease of operation is found in the side-by-side, flow-through chamber. With this chamber, random noise was largely eliminated by averaging over 10 s. However, systematic error due to non-idealities of the measurement system resulted in uncertainty in the time axis on the order of 10 s. Better time resolution was limited largely by imperfect fluorimeter cuvette mixing, as well as fluorimeter measurement noise, imperfect receptor chamber mixing, small time variations of tube flow rates, and deviations from plug flow in the tubing.

This study has developed expressions for deconvoluting transdermal flux from fluorescence signals. However, the approach is broadly applicable. Although side-by-side chambers have been used, the geometry of the chamber is irrelevant. Moreover, no assumptions based on transport across skin have been made. Instead, the flux of molecules into the receptor compartment is determined, without regard to the source of the molecules. The equations are valid for release of molecules into a receptor bath from any drug source (i.e., polymer matrices, hydrogels, liposomes, tissues). Thus, these methods for measurement of rapid release kinetics may be useful in transdermal and other types of drug delivery studies when time resolution on the order of one half minute is needed.

ACKNOWLEDGMENTS

We thank O. Malkova, R. Langer, S. S. Mitragotri, V. G. Bose, and E. A. Gift for helpful discussions and C. H. Liu and T. P. Singh for tissue preparation. This work was supported in part by the German Research Society (UP), Cygnus Therapeutic Systems (YAC, MRP, JCW), Army Research Office Grant DAAL03-90-G-0218 (JCW), and National Institutes of Health Grant GM34077 (JCW).

REFERENCES

1. R. L. Bronaugh and H. I. Maibach (eds.). *Percutaneous Absorption, Mechanisms—Methodology—Drug Delivery*. Marcel Dekker, New York, 1989.
2. J. Hadgraft and R. H. Guy (eds.). *Transdermal Drug Delivery: Developmental Issues and Research Initiatives*, Marcel Dekker, New York, 1989.
3. Z. Fehér, I. Kolbe, and E. Pungor. Application of flow-through techniques to drug dissolution studies. *Analyst* 116, 48–487 (1991).
4. M. Talukdar and J. A. Plaizier-Vercammen. Flow-through meth-

ods is advantageous for dissolution experiment of small dosage form. *Pharmazie* 47, 458–459 (1992).
5. E. R. Edelman, L. Brown, J. Taylor, and R. Langer. In vitro and in vivo kinetics of regulated drug release from polymer matrices by oscillating magnetic fields. *J. Biomed. Mater. Res.* 21, 339–353 (1987).
6. W. J. Addicks, G. L. Flynn, and N. Weiner. Validation of a flow-through diffusion cell for use in transdermal research. *Pharm. Res.* 4, 337–341 (1987).
7. S. W. Frantz, D. A. Dittenber, D. L. Eisenbrandt, and P. G. Watanabe. Evaluation of a flow-through in vitro skin penetration chamber method using acetone-deposited organic solids. *J. Toxicol—Cut. & Ocular Toxicol.* 9, 277–299 (1990).
8. J. Sclafani, J. Nightengale, P. Liu, and T. Kurihara-Bergstrom. Flow-through system effects on in vitro analysis of transdermal systems. *Pharm. Res.* 10, 1521–1526 (1993).
9. K. Knutson, S. L. Krill, W. J. Lambert, and W. I. Higuchi. Probing the structure of stratum corneum on the molecular level. In P. I. Lee and W. R. Good (eds.), *Controlled-Release Technology,* American Chemical Society, Washington D.C., 1987, pp. 241–266.
10. M. R. Prausnitz, V. G. Bose, R. Langer, and J. C. Weaver. Electroporation of mammalian skin: A mechanism to enhance transdermal drug delivery. *Proc. Natl. Acad. Sci. USA* 90, 10504–10508 (1993).
11. M. R. Prausnitz, U. Pliquett, R. Langer, and J. C. Weaver. Rapid temporal control of transdermal drug delivery by electroporation. submitted.
12. D. C. Chang, B. M. Chassy, J. A. Saunders, and A. E. Sowers. *Guide to Electroporation and Electrofusion,* Academic Press, New York, 1992.
13. J. C. Weaver. Electroporation: a general phenomenon for manipulating cells and tissues. *J. Cell Biochem.* 51, 426–435 (1993).
14. J. W. Furry. *Preparation, Properties and Applications of Calcein in a Highly Pure Form.* PhD Thesis, Iowa State University, Ames, IA, 1985.